Special Issue on Cell Biology

ARTICLE

Sporesight: A real-time computer vision-driven inference tool for pollen development stage classification in eggplant

John Albert M. Caraan*[1], Ariezel M. Bautista[2], John Benedict V. Lamorin[1], and Val Randolf M. Madrid[2]

[1]Institute of Plant Breeding, College of Agriculture and Food Science, University of the Philippines Los Baños, Los Baños, Laguna 4030, Philippines
[2]Institute of Computer Science, College of Arts and Sciences, University of the Philippines Los Baños, Los Baños, Laguna 4030, Philippines

ABSTRACT

Eggplant (*Solanum melongena* L.) is one of the major vegetable crops in the Philippines, significantly contributing to agricultural productivity and rural livelihoods. The economic contribution of this crop, valued at more than 9 billion pesos in 2024, underscores the need to continuously develop new and improved varieties that can adapt to the rapidly changing climate. One of the key strategies to expedite breeding activities leverages the use of doubled haploid technology, which requires the use of precise developmental stages of microspores or pollen for *in vitro* anther culture. This study presents *Sporesight*, a real-time, machine learning-driven desktop application designed to automate the classification of eggplant pollen developmental stages using object detection techniques. Initially, an expertly annotated dataset of 124 unique microscopic images, containing 3479 instances spanning seven distinct classes corresponding to eggplant microspore developmental stages, was used to train an AI model using the YOLOv5 algorithm. The model achieved a mean Average Precision (mAP@0.5) of 0.628, with high accuracy for morphologically distinct classes but moderate confusion for visually similar classes. This AI model was then integrated into an intuitive graphical user interface that provides image upload and preview, class-wise result visualization, and inference capabilities for the captured microscopic field of view, at an average time of 2.9 frames per second. As each captured microscopic field of view corresponded to a single frame, the system delivered inference results within 349 milliseconds. *Sporesight* provides high-throughput capabilities for selecting explants with suitable microspore developmental stages for *in vitro* culture, thereby contributing to streamlining the efforts to accelerate the development of climate-smart eggplant varieties.

*Corresponding author
Email Address: **jmcaraan1@up.edu.ph**
Date received: 17 October 2025
Dates revised: 08 December 2025
Date accepted: 02 January 2026
DOI: https://doi.org/10.54645/202619SupGZM-68

INTRODUCTION

In the Philippines, eggplant (*Solanum melongena* L.) is one of the major vegetable crops, contributing 228.27 thousand metric tons in total production volume and valued at more than 9 billion pesos in 2024 (Philippine Statistics Authority, 2024). Its production plays a significant role in Philippine agriculture, supporting both economic growth and livelihood security. Therefore, breeding new and improved varieties that address critical production challenges is key to sustaining bioeconomies, including the eggplant industry (Małyska & Jacobi, 2018).

One major prerequisite for a successful eggplant breeding program is the availability of pure, highly homozygous lines, which are used as parentals. Pure lines, or inbred lines, are traditionally generated via successive self-pollination of six to 10 generations (Mir et al., 2021). However, given the lengthy periods and high costs required to obtain homozygous parental lines, an alternative strategy is to produce doubled-haploid (DH) lines to shorten the breeding cycle. Androgenesis-based techniques, such as *in vitro* anther culture of microspores or pollen grains, are among the most widely used methods for producing DH lines by redirecting the developmental fate of male gametes toward a sporophytic pathway (Segui-Simarro, 2021).

The success of haploid induction techniques depends heavily on culture conditions, the genotype of the donor plant material, and the developmental stage of the microspores or pollen used for *in vitro* culture. In terms of culture conditions, the general composition of the culture medium and the application of heat stress treatment have largely remained consistent since the seminal work of Dumas de Vaulx & Chambonnet (1982), who established a reliable and reproducible protocol for haploid embryo induction and doubled haploid plant regeneration in eggplant. Their method

KEYWORDS

microspores, eggplant pollen development stages, computer vision, machine learning

involved incubating anthers in darkness at 35°C for 8 days, followed by culturing at 25°C in a medium supplemented with 2,4-D and kinetin to promote the formation of microspore-derived embryos (MDEs).

Meanwhile, the genotype-dependent response of eggplant anthers to *in vitro* culture has also been extensively studied (Başay & ElliAltioğlu, 2013; Bat et al., 2022; Rivas-Sendra et al., 2017). In these studies, the differential sensitivities of the various eggplant genotypes to androgenesis were attributed to the unique genetic, hormonal, and physiological background of the donor tissues, suggesting that the success of an *in vitro* anther culture is not solely determined by the culture conditions but also by the intrinsic biological state of the explant during the culture initiation.

The developmental stage of microspores or pollen at the time of anther excision and culture initiation is another major factor influencing the rate of MDE formation. It is generally accepted that the most responsive stage corresponds to the period around the first pollen mitosis, when the microspores begin to develop vacuoles and form young bicellular pollen (Mir et al., 2021; Rotino, 2016; Salas et al., 2012). Morphological indicators such as bud and anther lengths are commonly used to approximate the developmental stage of microspore or pollen within the anther locules; however, this approach does not provide an absolute determination of their exact stage.

Cytological characterization of anthers containing inducible developmental stages of microspores or pollen is often required to ensure the use of appropriately staged donor materials for culture initiation (Mir et al., 2021; Rotino, 2016; Salas et al., 2012). This process, however, demands a high level of technical expertise and typically involves routine use of toxic or hazardous staining reagents such as acetocarmine or fluorescent dyes like DAPI (4′,6-diamidino-2-phenylindole) and FDA (Fluorescein Diacetate), which require an expensive epifluorescence microscope for viewing. These limitations underscore the need for automated and precise tools that can reliably determine microspore and pollen developmental stages while reducing technical burden and subjectivity.

Convolutional Neural Networks (CNNs), a cornerstone of deep learning, have shown remarkable success in image classification and object detection tasks by automatically learning hierarchical features from raw image data. As demonstrated by García-Fortea et al. (2020) through the Microscan system, these approaches can accurately and efficiently identify pollen developmental stages with minimal human intervention. Despite the success of deep learning in microspore characterization, several critical gaps remain, which prevent its widespread adoption in routine breeding workflows.

First, the existing system operates as a post-processing tool that requires high-performance computing; thus, it lacks the capability for real-time inference directly from microscope feeds during live screening. Second, there is a scarcity of user-friendly software interfaces that bridge the gap between complex AI architectures and laboratory technicians who may lack programming expertise. Third, the dataset of the existing system is not publicly available, and the models were trained on foreign germplasm, limiting their generalization to the specific local genotypes used in Philippine breeding programs. To expound, while the Microscan system yielded highly accurate predictions (0.863 mAP), it used the RetinaNet architecture, which is typically computationally intensive and designed for high-throughput batch analysis. In similar studies comparing the performance of various object detection algorithms, RetinaNet performed at only up to a third of the frames per second of You Only Look Once (YOLO) (Tan et al., 2021; Yinkfu et al., 2025). This system was also presented primarily as a research methodology, with unclear guidance on how non-expert end users can use it with no extensive knowledge of computer programming. Regarding data annotation, Microscan relied on custom labeling workflows (an undisclosed software developed by a Spanish company called SomData Analytics) that are not readily available as open-source tools.

To address the challenges mentioned, we developed an integrated microspore characterization platform called *Sporesight*. Here, we took a different approach to creating a machine learning–driven computer vision inference system using YOLOv5. We then integrated our machine learning model into an intuitive graphical user interface to automate the complex characterization of microspore and pollen developmental stages, tailored to the biological nuances of eggplants grown in the Philippines. Our approach ensured that our model captured the specific microspore or pollen morphology of the genotype we used, which may differ from that of the accessions used in the previous European study.

MATERIALS AND METHODS

Sporesight's development pipeline followed a sequential workflow, beginning with eggplant material establishment and microscopic image acquisition, during which microspore and pollen images were collected and expertly annotated to generate training data. The annotated dataset was used to train the machine learning model, with iterative validation to optimize hyperparameters and ensure robust generalization, followed by performance evaluation using an independent test set. The validated model was then deployed onto a target inference platform and integrated into a user-friendly desktop application to enable real-time prediction of pollen developmental stages (Figure 1).

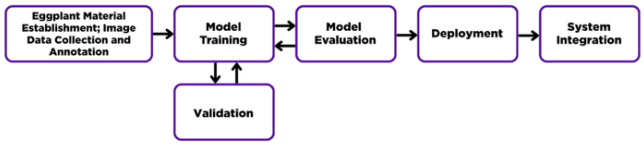

Figure 1: Development pipeline for the real-time machine learning-driven computer vision inference system for eggplant pollen developmental stages.

Establishment of Plant Materials, Image Dataset Collection, and Annotation

Donor eggplant plants (cv. Mistisa; acc. PH11424) were grown under controlled screenhouse conditions at the Institute of Plant Breeding, College of Agriculture and Food Science, University of the Philippines Los Baños. Solitary floral buds of varying sizes were randomly collected from ten (10) different plant replicates to ensure representative sampling. Upon dissection, anthers were immediately squashed on clean glass slides and examined under a phase-contrast microscope (Olympus CKX53). For each sample, five randomly selected microscopic fields were captured at 40× objective magnification. The resulting images and instances were individually annotated using LabelImg, a Python-based graphical annotation tool, following the morphological descriptors reported by Salas *et al.* (2012) (Table 1).

Table 1: Summary of distinct features of different microsporeand pollen developmental stages (Tetrads, Young Microspore, Mid-Vacuolate Microspore, Young Bicellular Pollen, Mid-late Bicellular Pollen, Mature Pollen), as described by Salas *et al.* (2011).

DEVELOPMENTAL STAGE	DISTINCT FEATURES
Tetrads	Tetrad of cells enclosed in a thick, callose envelope
Young microspore	Free, unicellular microspores with polygonal shape, thin cell wall, and reduced size; large, and central nucleus
Mid-Vacuolate Microspore	Free, unicellular microspores with thicker cell walls, rounder shape, and increased diameter; vacuolization may be visible
Late/Vacuolate microspore	Free, unicellular microspores with a well-developed cell wall, off-centered nucleus, and are larger in diameter; the presence of a large, cytoplasmic vacuole
Young Bicellular Pollen	Round-shaped and relatively bigger in size; has two different nuclei
Mid-late Bicellular Pollen	Larger in size, has a cytoplasmic vacuole, with one nucleus migrating at the center; increased opacity
Mature Pollen	High opacity, has a centered nucleus, remarkably denser; appears nearly black under a phase contrast microscope

One hundred twenty-four (124) unique images, with approximately 20 microspores per microscopic field of view, were collected and annotated using the established descriptors. Annotations were categorized into seven distinct developmental classes: tetrad, young microspore, mid microspore, late microspore, young pollen, mid-late pollen, and mature pollen. To minimize misclassification, deformed structures, imaging debris, and artifacts were consolidated into a single category designated as 'others'.

A separate test dataset consisting of 78 images was withheld from the training process to validate the AI model. The images from this test dataset also contained at least 20 instances for each of the seven developmental classes, as well as the 'others' category, to ensure balanced evaluation across all stages

Development Tools Used

The model training and validation processes were conducted on a machine equipped with an NVIDIA® GTX 1070 GPU (6 GB VRAM), 16 GB of RAM, and a 12-core Intel® Core™ i7 processor (2.5 GHz). For real-time image acquisition, a ToupTek® XCAM1080PHB camera was mounted onto the Olympus® phase-contrast microscope. Development and integration of the final application were carried out on a laptop with an AMD® Ryzen™ 9 processor and 32 GB RAM.

Sporesight was developed using Python 3.9.6 and PyTorch 2.0, with Visual Studio Code™ as the primary development environment. Core dependencies included OpenCV 4.11.0 for microscope camera image acquisition, PySide6 6.9.0 for graphical user interface development, ONNX Runtime 1.19.2 for real-time model inference, and NumPy 1.26.4 for numerical operations.

Although the YOLOv8 architecture was initially evaluated, YOLOv5 was selected for final deployment due to its greater compatibility with the required OpenCV–PyQt integration pipeline and its more stable ONNX export workflow at the time of development. These considerations were vital given the need for a reliable, real-time inference system that could interface directly with microscope camera hardware within a desktop application. In addition, YOLOv5 exhibited fewer dependency conflicts with the specific library versions required for image acquisition and GUI rendering, enabling a more robust and reproducible deployment. While model training was performed on a high-performance workstation, the final application was designed to run efficiently on standard laboratory desktop computers with limited computational resources, ensuring accessibility and stable performance for routine use by researchers and technicians.

Model Training and Hyperparameters

The annotated dataset was used to train a YOLOv5 object detection model using the Ultralytics framework, and the resulting model used the following hyperparameters, summarized in Table 2. Input images were resized to 640×640 pixels to match the model's expected input dimensions.

Table 2: YOLOv5 training and optimization configuration hyperparameters.

Parameter	Value
Batch	64
Sub-divisions	64
Learning Rate	0.001
Momentum	0.949
Decay	0.0005
Data Augmentation	Mosaic, HSV adjustments (saturation: 1.5, exposure: 1.5, hue: 0.1)

AI Model Training Pipeline

The process began with dataset preparation, where annotated images from UPLB-IPB were preprocessed and structured for YOLO training. The YOLOv5 model was iteratively trained and validated using custom scripts, with each iteration refining detection accuracy and class sensitivity. Once performance benchmarks were achieved, the trained model was converted to the ONNX format and integrated into the desktop application for real-time inference.

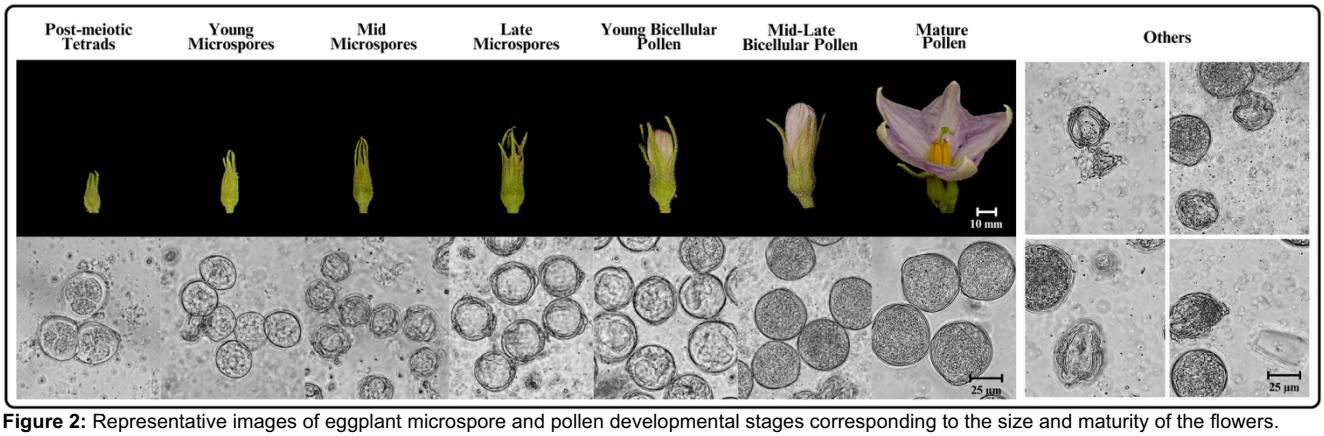

Figure 2: Representative images of eggplant microspore and pollen developmental stages corresponding to the size and maturity of the flowers.

Evaluation of the Model

The YOLOv5 model was evaluated using precision and recall—two key metrics for object detection systems. A precision-recall (PR) curve was used to visualize the trade-off between these metrics across different confidence thresholds. This allowed for fine-tuning of the model to ensure optimal detection sensitivity and specificity, especially across closely related stages of microspore development (Huda, 2024).

RESULTS AND DISCUSSION

Dataset Characteristics

During the course of the study, we collected and individually annotated a total of 3479 eggplant microspores and pollen, with the following class distribution: 106 tetrads, 851 young microspores, 478 mid microspores, 268 late microspores, 167 young pollen, 786 mid-late pollen, and 358 mature pollen. We also noted 465 debris, artifacts, and deformed structures across the image dataset. The representative images of various eggplant microspore and pollen morphologies in developing floral organ structures are shown in Figure 2.

Owing to the inherent developmental asynchrony of microspores and pollen within floral tissues, the resulting dataset exhibited an uneven class distribution. Such imbalance can bias model predictions toward more frequently represented classes (Leevy et al., 2018); however, the observed class ratios fall well below the thresholds commonly associated with severe class imbalance (majority-to-minority ratios of 100:1 to 10,000:1) as defined by He and Garcia (2009). Consequently, the dataset was deemed suitable for training and used to establish a proof-of-concept model.

AI Model Training and Deployment

The microspore classification model developed with YOLOv5 was evaluated on the designated test set using the confusion matrix and precision-recall (PR) curve metrics. Such metrics provide a comprehensive understanding of the model's performance across per-class accuracy, precision, and recall. The overall results are summarized in Table 3.

Table 3: Per-class performance metrics of the YOLOv5 model for eggplant microspore and pollen classification. Precision, recall, and F1 scores are computed at a confidence threshold of 0.5, while AP (Average Precision) represents the area under the precision-recall curve.

Class	Precision	Recall	F1 Score	AP
Tetrad	0.6634	0.9710	0.7882	0.935
Young Microspore	0.5050	0.3054	0.3806	0.934
Mid Microspore	0.3232	0.2254	0.2656	0.545
Late Microspore	0.2020	0.4878	0.2857	0.301
Young Pollen	0	0	0	0.450
Mid-late Pollen	0.5500	0.3022	0.3901	0.687
Mature Pollen	0.4900	0.4188	0.4516	0.323
Others	0.8100	0.6864	0.7431	0.847
Mean	0.4429	0.4246	0.4131	0.628

Confusion Matrix Analysis

The confusion matrix revealed differential classification performance across different pollen developmental stages (Figure 3). The YOLOv5 model achieved high recall for visually distinct classes, including the others category (81%) and the tetrad stage (67%). In contrast, substantial misclassification occurred between classes representing adjacent developmental stages. Notably, 49% of young microspores were misclassified as mid microspores, while 55% of mid microspores were predicted as young microspores. A similar reciprocal confusion was observed between mid–late pollen and mature pollen, with nearly half of the instances in each class misidentified as the other (Figure 3).

These misclassifications likely reflect the fine-grained, continuous nature of microspore and pollen development, in which adjacent stages exhibit subtle morphological differences that are difficult to resolve visually. Developmental asynchrony within individual anthers further contributes to overlapping phenotypic features among stages (Salas et al., 2012; Adhikari & Kang, 2017; Pagalla,

2023). Nonetheless, this behavior does not undermine the intended application of the model for identifying stage ranges suitable for *in vitro* culture; instead, the tendency to interchange predictions between neighboring stages captures biologically meaningful transitions rather than enforcing artificially discrete class boundaries. Overall, the confusion matrix suggests that the primary limitation lies in the inherent visual similarity of adjacent developmental stages, highlighting the potential benefit of merging ambiguous classes and improving dataset balance in future iterations.

Figure 3: Confusion matrix of the YOLOv5 model illustrating actual vs. predicted classification rates for pollen developmental stages.

Precision-Recall (PR) Analysis

The Precision-Recall (PR) curve (Figure 4) extends the confusion matrix by showing how model confidence varies across classes. With a mAP@0.5 of 0.628, the model shows moderate success but exhibits apparent performance differences. It performs best on visually distinct stages, such as the tetrad (0.935 AP) and young microspore (0.934 AP), where it maintains high precision. However, it struggles on similar-looking stages, such as the late microspore (0.301 AP) and mature pollen (0.323 AP); for these classes, any gain in recall results in a sharp drop in precision. When combined with the confusion matrix, these results reveal a deeper trend: even for high-scoring classes such as the young microspore, the model often makes high-confidence errors, frequently misclassifying mid microspores. This pattern of confident misidentification also appears in the mid-late and mature pollen stages.

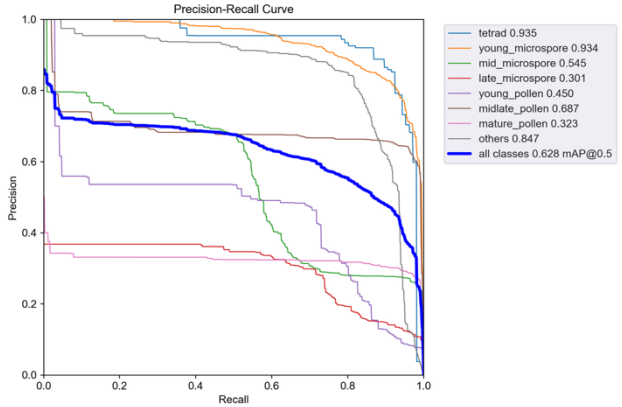

Figure 4: Precision-Recall performance across various pollen developmental stages, showing high precision for the tetrad and young microspore classes contrasted against lower performance in late microspore and mature pollen stages.

In terms of practical utility, the observed ambiguity and imprecision between developmentally close microspore and pollen classes have minimal negative impact on the model's intended application. In practice, anthers containing young to mid microspore stages are typically selected for *in vitro* culture, as these developmental phases naturally progress toward the inducible late microspore to young bicellular pollen stages during culture incubation (Salas et al., 2012). This means that even if the model occasionally fails to distinguish young from mid microspores, it would still effectively identify anthers within the optimal developmental window for androgenic induction. Meanwhile, discrepancies in discrimination between the late and mature pollen stages are not particularly critical, as these stages are already differentiated and not amenable to *in vitro* culture. The observed classification overlaps remain acceptable and do not compromise the model's practical value for guiding explant selection for *in vitro* anther and isolated microspore culture experiments.

The overall results highlight the viability of using machine learning, specifically YOLOv5, for classifying the developmental stages of eggplant microspores and pollens. The model demonstrated acceptable overall accuracy, with mAP@0.5 = 0.628, which aligns with the performance expectations for complex microscopic classification tasks involving morphologically similar cases. Microscopic image detection mAP values vary widely depending on task complexity and specificity, ranging from approximately 24% for mixed cell-instance segmentation across 30 heterogeneous classes to over 95% for specialized single-cell-type detection tasks.

For tasks involving morphologically distinct cell types, recent studies have reported substantially higher mAP values. For instance, leukemia cell detection in bone marrow microscopy achieved mAP values of 95.9% for acute lymphoblastic leukemia and 98.6% for chronic lymphocytic leukemia using a spatially-guided learning network (Mei et al., 2025). On the other hand, findings from Sazak and Kotan (2024) show that blood cell classification tasks using YOLO architectures have similarly reported mAP values exceeding 93% when discriminating between visually distinct cell categories such as red blood cells, white blood cells, and platelets. However, these high-performance results reflect the detection of clearly differentiated cell types rather than the fine-grained discrimination of temporal stages within a continuous biological process.

In more comparable scenarios involving subtle morphological distinctions, performance metrics are considerably lower. Sperm detection in testicular biopsy images achieved a mAP of 74.1% using a two-stage deep detection pipeline (Wu et al., 2021). Similarly, histopathology nuclei segmentation tasks have reported mAP values of 38-39% on breast tissue datasets (Lagree et al., 2021), while mixed microscopy cell segmentation across 30 diverse classes achieved a mean average precision of only 24.37% (Khalid et al., 2021). These benchmarks highlight the inherent difficulty of microscopic classification tasks where visual similarity between classes is high and morphological boundaries are ambiguous.

Given that our classification task involves discriminating between adjacent developmental stages with subtle morphological differences, the observed mAP@0.5 of 0.628 represents acceptable performance for this proof-of-concept study. It falls within the mid-to-upper range of comparable fine-grained microscopic classification tasks. The model demonstrated robust performance across morphologically distinct classes, such as the tetrad and young microspore. Conversely, performance on visually similar classes such as late microspore (AP 0.301) and mature pollen (AP

0.323) was substantially lower, reflecting the inherent difficulty of discriminating between closely related developmental stages.

The misclassifications observed between visually indistinguishable stages (e.g., young_microspore vs. mid_microspore) underscore limitations in feature representation—a challenge frequently encountered in microscopic image classification where intra-class variance and inter-class similarity are pronounced due to the constraints produced by the restrictions in viewpoints from which the microscope images are captured (Venkataramanan et al., 2021).

Desktop Application Development

Integrating the AI prediction model into a user-friendly desktop graphical interface is essential to translate YOLOv5's computational power into a practical, accessible tool for bench researchers and laboratory technicians engaged in *in vitro* anther culture experiments. To this end, we developed an intuitive application that allows users to seamlessly deploy the trained AI model, interface directly with a microscope, and analyze the microspores and pollen in the captured microscopic field of view in real time. This integration bridges the gap between advanced machine learning models and routine laboratory workflows, which enables data-driven decision-making for *in vitro* anther culture explant selection. *Sporesight* employs a modular architecture comprising five core components, as detailed in the Supplemental Material.

Application Interface and Functionality

Sporesight consists of three core functional components: the Configuration page, the Camera View page, and the Analytics page, as detailed in the succeeding sections.

1. Configuration Page

This page enables users to configure the system by uploading the trained model (in ONNX format) and a text file containing class labels. It also includes controls for adjusting the confidence threshold and provides a real-time preview of the model and class setup (Figure 5).

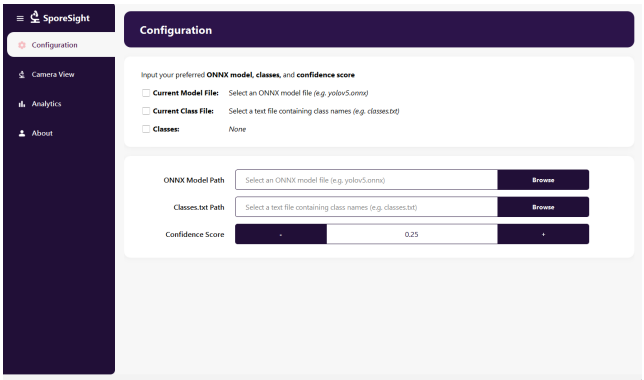

Figure 5: Configuration Page of Sporesight where the AI model, classifications, and confidence scores are defined by the user.

2. Camera View Page

This page displays the live feed from the microscope camera, provided the device is connected to the IP camera's Wi-Fi hotspot. It also shows a preview of the selected model and its classes, and enables inference using the ONNX Runtime. Upon completion of the inference, a dialog appears allowing users to save or discard the image with the detected objects (Figure 6).

Figure 6: Camera View Feed View Page (with connection).

3. Analytics Page

The analytics page presents a summary of detected objects from saved images. Users can review and delete individual detection records. Clicking any card opens a detailed view dialog displaying the full-resolution annotated image, a table of detected classes with frequency counts and confidence ranges visualized as progress bars, and options to delete individual records (Figure 7). The page header displays the total detection count, updating dynamically asusers add or remove detections. The Analytics page also includes a "Detect an image" button that lets users upload static images for inference, providing an alternative to the live camera feed workflow. When date folders become empty after deletion operations, the system automatically removes them to maintain organization.

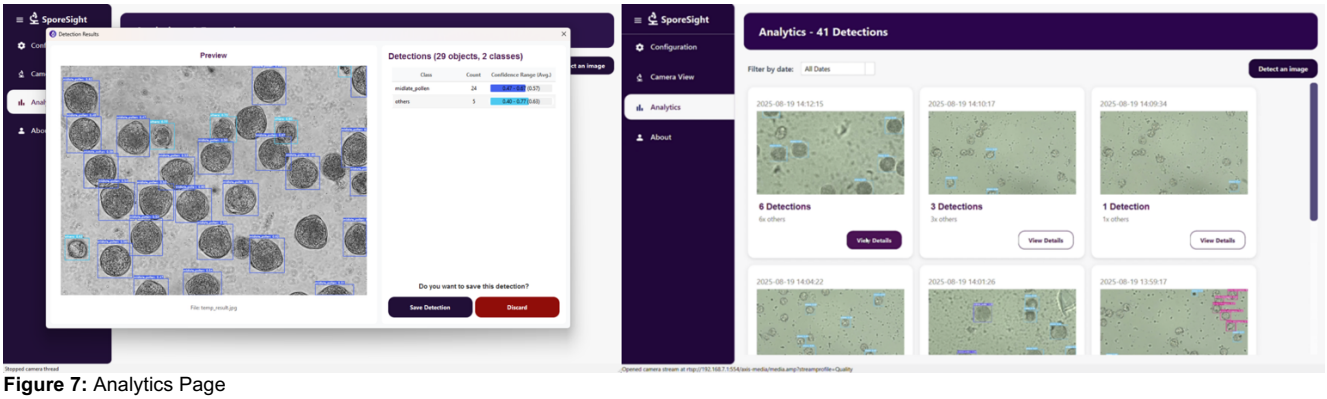

Figure 7: Analytics Page

Performance Evaluation

To validate *Sporesight's* real-time capabilities, we conducted inference speed benchmarks on a MacBook Air with an Apple M2 chip (8-core CPU, 8-core GPU, 8 GB unified memory). Performance measurements were conducted using a representative test image (1920×1080 resolution) processed through the complete detection pipeline. The YOLOv5 model resized input images to

640×640 pixels for inference, with a confidence threshold set to 0.25. We performed 100 consecutive inference iterations after a 10-iteration warm-up to ensure stable performance metrics. Each iteration included complete processing: ONNX Runtime inference execution and post-processing operations (confidence filtering, bounding box extraction, and non-maximum suppression). As a result, the MacBook Air M2 achieved an average processing time of approximately 349 ms per frame, corresponding to 2.9 FPS, validating its real-time capability (Table 4).

Table 4: Inference performance benchmarks of *Sporesight*.

Hardware Configuration	Image Resolution	Inference + Post-processing (ms)	FPS
MacBook Air M2 (8-core CPU/GPU), 8GB RAM	1920×1080 → 640×640	348.88 ± 22.11 ms	2.9

Operational Requirements

Users must prepare two essential configuration files to operate *Sporesight*:

1. Class Labels File (classes.txt): A plain text file containing class names for pollen developmental stages, with one class per line. The number of classes in this file must exactly match the number of output classes in the trained ONNX model. Example format:

```
tetrad
young_microspore
mid_microspore
late_microspore
young_pollen
midlate_pollen
mature_pollen
others
```

2. ONNX Model File ([model_name].onnx): The trained YOLOv5 model exported in ONNX format. Pre-trained models for rice are available from the project repository.

Application Installation Packages

The *Sporesight* application installation packages are currently available only upon request. Once the appropriate Intellectual Property Rights protection has been secured, *Sporesight* will be made publicly available and compatible for Windows and Mac operating systems in an executable form.

CONCLUSION

This study developed *Sporesight*, a real-time, desktop-compatible microspore and pollen classification application that uses machine learning to automate the identification of eggplant anthers at optimal developmental stages for *in vitro* culture. By integrating a YOLOv5-based object detection model with a microscope-mounted camera, the system provides researchers at UPLB-IPB with an efficient and scalable tool for data-driven explant selection. Evaluation results generally demonstrated acceptable accuracy (mAP@50 = 0.628), particularly in stages with distinct morphological features, and highlight areas for improvement in classifying visually similar stages. For future releases, our team will build a more robust training dataset to improve the model's accuracy and precision. Imbalanced class distributions are expected; hence, we will attempt to instruct the model to pay more attention to minority classes to reduce inference bias against underrepresented groups. We will also merge and consolidate biologically distinct classes into subgroups according to established eggplant microspore morphologies that are amenable to either anther or isolated microspore culture experiments.

Overall, *Sporesight* addresses a critical bottleneck in doubled haploid production and makes a significant contribution to the advancement of crop breeding technologies. Future work should focus on expanding the training dataset, improving model precision, enhancing the database and data analytics, and optimizing system usability to support broader implementation in agricultural biotechnology research.

ACKNOWLEDGMENTS

This study was made possible through the grant provided by the Department of Science and Technology - Philippine Council for Agriculture, Aquatic, and Natural Resources Research and Development (DOST-PCAARRD) to the University of the Philippines Los Baños (UPLB) led by Mr. John Albert M. Caraan (Fund Code: N9-357-21/ N9-357-2A) on the "Utilization of Interdisciplinary Strategies and Plant Breeding Innovations for the Development of Eggplant (*Solanum melongena* L.) Haploid and Doubled Haploid Lines". The team also acknowledges Dr. Jose María Seguí Simarro of the Universitat Politècnica de València, Spain, for the technical guidance and masterclasses on microsporogenesis and doubled haploids as part of his consultancy duties. We also thank Ms. Lorisabelle Sebastian for the provision of microscopic images as part of her undergraduate thesis (to be published as separate journal article). Lastly, we acknowledge our Laboratory and Administrative staff, Ms. Rowena Frankie, Ms. Marilyn de Vera, Mr. Frances Elecion, Mr. Cris Urriza, and Mr. Elmer Doria, for the support they provided during the study.

CONFLICT OF INTEREST

The authors declare that there is no conflict of interest.

CONTRIBUTIONS OF INDIVIDUAL AUTHORS

JAMCaraan conceptualized the system and all authors contributed to the design and execution of the study. JVBLamorin and JAMCaraan performed the data curation and expert annotation. VRMMadrid and AMBautista performed the model training and evaluation. AMBautista designed and developed the graphical user interface with the executive guidance of JAMCaraan and VRMMadrid. All authors, led by JAMCaraan, contributed and finalized the manuscript.

REFERENCES

Adhikari, P., & Kang, W. (2017). Association of Floral Bud and Anther Size with Microspore Developmental Stage in Campari Tomato. *Horticultural Science and Technology*, *35*, 608–617. https://doi.org/10.12972/kjhst.20170065

Başay, S., & ElliAltioğlu, Ş. Ş. (2013). Effect of genotypical factors on the effectiveness of anther culture in eggplant (Solanum melongena L.). *TURKISH JOURNAL OF BIOLOGY*, *37*, 499–505. https://doi.org/10.3906/biy-1210-38

Bat, H., Altindağ, F. N., YiĞiT, M. A., ElliAltioğlu, Ş. Ş., & ÇmlekçiOğlu, N. (2022). Genotype Effect as One of the Affecting Factors on the Success of Anther Culture in Eggplant (Solanum melongena L.). *Horticultural Studies*, *39*(2), 41–47. https://doi.org/10.16882/hortis.1119745

Chen, E., Shalaginov, M. Y., Liao, R., & Zeng, T. H. (2022). Real-time Detection of Acute Lymphoblastic Leukemia Cells Using Deep Learning. BioRxiv (Cold Spring Harbor Laboratory). https://doi.org/10.1101/2022.10.22.513362

García-Fortea, E., García-Pérez, A., Gimeno-Páez, E., Sánchez-Gimeno, A., Vilanova, S., Prohens, J., & Pastor-Calle, D. (2020). A Deep Learning-Based System (Microscan) for the Identification of Pollen Development Stages and Its Application to Obtaining Doubled Haploid Lines in Eggplant. *Biology*, *9*(9), 272. https://doi.org/10.3390/biology9090272

Halenur Sazak, & Muhammed Kotan. (2024). Automated Blood Cell Detection and Classification in Microscopic Images Using YOLOv11 and Optimized Weights. *Diagnostics*, *15*(1), 22–22. https://doi.org/10.3390/diagnostics15010022

He, H., & Garcia, E. A. (2009). Learning from Imbalanced Data. *IEEE Transactions on Knowledge and Data Engineering*, *21*(9), 1263–1284. https://doi.org/10.1109/TKDE.2008.239

Huda, N. U. (2024, September 17). Precision Recall Curves. *Train in Data's Blog*. https://www.blog.trainindata.com/precision-recall-curves/

Jia, Y., Lu, C., Li, X., Ma, M., Pei, Z., Sun, Z., & Chen, Y. (2021). *Nuclei Instance Segmentation and Classification in Histopathological Images using a DT-Yolact*. https://doi.org/10.1109/iucc-cit-dsci-smartcns55181.2021.00072

Khalid, N., Munir, M., Edlund, C., Jackson, T. R., Trygg, J., Sjögren, R., Dengel, A., & Ahmed, S. (2021). *DeepCIS: An end-to-end pipeline for cell-type aware instance segmentation in microscopic images*. 1–4. https://doi.org/10.1109/BHI50953.2021.9508480

Lagree, A., Mohebpour, M., Meti, N., Saednia, K., Lu, Fang-I., Slodkowska, E., Gandhi, S., Rakovitch, E., Shenfield, A., Sadeghi-Naini, A., & Tran, W. T. (2021). A review and comparison of breast tumor cell nuclei segmentation performances using deep convolutional neural networks. *Scientific Reports*, *11*(1), 8025. https://doi.org/10.1038/s41598-021-87496-1

Leevy, J. L., Khoshgoftaar, T. M., Bauder, R. A., & Seliya, N. (2018). A survey on addressing high-class imbalance in big data. *Journal of Big Data*, *5*(1), 42. https://doi.org/10.1186/s40537-018-0151-6

Małyska, A., & Jacobi, J. (2018). Plant breeding as the cornerstone of a sustainable bioeconomy. *New Biotechnology*, *40*, 129–132. https://doi.org/10.1016/j.nbt.2017.06.011

Mei, L., Lian, C., Han, S., Ye, Z., Hua, Y., Sun, M., He, J., Ye, Z., Mei, M., Yaxiaer Yalikun, Shen, H., Lei, C., & Xiong, B. (2025). High-efficiency spatially guided learning network for lymphoblastic leukemia detection in bone marrow microscopy images. *Computers in Biology and Medicine*, *196*(Pt B), 110860–110860. https://doi.org/10.1016/j.compbiomed.2025.110860

Mir, R., Calabuig-Serna, A., & Seguí-Simarro, J. M. (2021). Doubled Haploids in Eggplant. *Biology*, *10*(7), Article 7. https://doi.org/10.3390/biology10070685

Pagalla, D. B. (2023). Stages of Microspore Development in Eggplant (Solanum melongena L.). *BIOEDUSCIENCE*, *7*(1), 68–72. https://doi.org/10.22236/jbes/7111357

Philippine Statistics Authority (2024). Major Vegetable Crops Bulletin. Retrieved December 15, 2024, from https://psa.gov.ph/vegetable-root-crops/eggplant

Rivas-Sendra, A., Campos-Vega, M., Calabuig-Serna, A., & Seguí-Simarro, J. M. (2017). Development and characterization of an eggplant (Solanum melongena) doubled haploid population and a doubled haploid line with high androgenic response. *Euphytica*, *213*(4), 89. https://doi.org/10.1007/s10681-017-1879-3

Rotino, G. L. (2016). Anther Culture in Eggplant (Solanum melongena L.). In M. A. Germana & M. Lambardi (Eds.), *In Vitro Embryogenesis in Higher Plants* (Vol. 1359, pp. 453–466). Springer New York. https://doi.org/10.1007/978-1-4939-3061-6_25

Salas, P., Rivas-Sendra, A., Prohens, J., & Seguí-Simarro, J. M. (2012). Influence of the stage for anther excision and heterostyly in embryogenesis induction from eggplant anther cultures. *Euphytica*, *184*(2), 235–250. https://doi.org/10.1007/s10681-011-0569-9

Segui-Simarro, J. M. (Ed.). (2021). *Doubled Haploid Technology: Volume 2: Hot Topics, Apiaceae, Brassicaceae, Solanaceae* (Vol. 2288). Springer US. https://doi.org/10.1007/978-1-0716-1335-1

Tan, L., Huangfu, T., Wu, L., & Chen, W. (2021). Comparison of RetinaNet, SSD, and YOLO v3 for real-time pill identification. *BMC Medical Informatics and Decision Making*, *21*(1), 324. https://doi.org/10.1186/s12911-021-01691-8

Vaulx, R. D. D., & Chambonnet, D. (1982). Culture in vitro d'anthères d'aubergine (Solanum melon- gena L.): Stimulation de la production de plantes au moyen de traitements à + 35 °C associés à de faibles teneurs en substances de croissance. *Agronomie*, *2*(10), 983–988. https://doi.org/10.1051/agro:19821011

Venkataramanan, A., Laviale, M., Figus, C., Usseglio-Polatera, P., & Pradalier, C. (2021). Tackling Inter-class Similarity and Intra-class Variance for Microscopic Image-Based Classification. In M. Vincze, T. Patten, H. I. Christensen, L. Nalpantidis, & M. Liu (Eds.), *Computer Vision Systems* (pp. 93–103). Springer International Publishing. https://doi.org/10.1007/978-3-030-87156-7_8

Wu, D., Badamjav, O., Reddy, V., Eisenberg, M., & Behr, B. (2021). A preliminary study of sperm identification in microdissection testicular sperm extraction samples with deep convolutional neural networks. *Asian Journal of Andrology*, *23*(2), 135. https://doi.org/10.4103/aja.aja_66_20

Yinkfu, N., Nwovu, S., Kayizzi, J., & Uwamahoro, A. (2025). *Comparative Analysis of YOLOv5, Faster R-CNN, SSD, and RetinaNet for Motorbike Detection in Kigali Autonomous Driving Context*. https://doi.org/10.48550/ARXIV.2510.04912